

Material yielding and irreversible deformation mediated by dislocation motion

M.-Carmen Miguel^{1,a}, L. Laurson², and M.J. Alava²

¹ Departament de Física Fonamental, Facultat de Física, Universitat de Barcelona, Diagonal 647, 08028 Barcelona, Spain

² Laboratory of Physics, Helsinki University of Technology, P.O. Box 1100, 02015 HUT, Finland

Received 30 November 2007 / Received in final form 28 March 2008

Published online 21 May 2008 – © EDP Sciences, Società Italiana di Fisica, Springer-Verlag 2008

Abstract. We study the collective behavior of dislocation assemblies in simplified models of plastic deformation. We first review several numerical results on long range dislocation interactions with simplified dislocation motion constraints. These typically give rise to a yielding transition separating stationary and moving dislocation phases. Furthermore, we discuss the intermittent relaxation of the plastic strain-rate observed around this transition at mesoscopic scales, and how this intermittent behavior gives rise to an average slow power law relaxation in time known in the literature as Andrade's creep. We analyze the coherent dynamics and the average stress-strain relationship in the steady regime of plastic deformation. In this steady regime, plastic deformation proceeds in the form of plastic avalanches whose size and duration are broadly distributed and statistically characterized. One signature of the time correlations of this heterogeneous collective dislocation dynamics is a power spectrum scaling with frequency as $f^{-\alpha}$ with an exponent α close to 1.5. This feature appears to be peculiar of dislocation and grain boundary motion as has been observed in other physical situations in the vicinity of a yielding transition.

PACS. 62.20.-x Mechanical properties of solids – 62.20.Fe Deformation and plasticity

1 Introduction

In materials science, the general concept of yielding implies that the amount of force or stress applied to a material is above its characteristic yield strength which causes plastic flow or irreversible deformation. Thus the yield strength (or the yield point) should separate the two different regimes of elastic or reversible deformation, when the strain caused in the material will disappear once the force is removed, and that of plastic deformation after which some fraction of the induced strain will be permanent and non-reversible. Both crystalline and amorphous solids undergo plastic deformation under certain conditions. Crystals deform irreversibly due to the collective motion of dislocations. On the other hand, the microscopic mechanisms responsible for plastic flow in amorphous materials are, as yet, not so well understood. The yield stress of a crystal depends on several quantities such as dislocation density or temperature. Likewise, the yield stress of an amorphous material may depend on density, temperature, effective temperature, or other relevant variables.

In the past decade, it has been repeatedly reported that the mechanical and rheological properties of various amorphous materials, from foams to granular media,

at high densities and under low driving forces exhibit common features despite their constitutive and microstructural differences. A new kind of phase transition, the jamming transition, and the jamming concept was proposed to comprehend the observed phenomenology, which in some aspects resembles the behavior of glassy materials. On approaching the jamming transition, the dynamics becomes very slow and strongly heterogeneous in space and time. Well below the jamming threshold it appears as completely frozen. In the last few years a great effort has been devoted to the characterization of this jamming or yielding, if coming from the jammed phase, transition [1–4]. Foams under low shear rate deformation will initially stretch elastically until a critical value of the strain is reached, the yield strain, above which their flow will proceed in the form of heterogeneous bubble rearrangements [5]. Confined granular media under slow shear and near jamming conditions exhibit similar heterogeneous dynamics in space and time [6]. In this respect, exciting new pieces of experimental evidence seem to indicate that the jamming transition appears to be a critical phenomenon with universal features. In reference [7] growing time and dynamical length scales have been, for instance, recently measured in an air-driven granular material.

^a e-mail: carmen.miguel@ub.edu

Dislocation assemblies in crystalline matter belong to the broad class of systems that are governed by the presence of kinetic constraints (induced by interactions, geometry, and disorder), and are thus susceptible to undergo a yielding transition. Dislocations are quanta of plastic deformation. Their mutual interactions together with their dynamic constraints, which tie the motion of dislocations to their slip planes, lead to the possibility of forming metastable jammed configurations even in the absence of any disorder in the material. Thus the flow dynamics in crystal plasticity turns out to be qualitatively similar to that observed in some amorphous materials near jamming. Indeed, heterogeneous and intermittent deformation processes have been recently reported in the mechanical response of crystals at various length scales. Acoustic emission experiments of macroscopic ice single crystals [8,9] and ice polycrystals [10] under constant load (creep tests) show that their plastic deformation proceeds as a series of intermittent bursts of activity, in response to dislocation multiplication and annihilation processes, or corresponding to collective dislocation rearrangements. A statistical analysis of the intensity of the acoustic events was performed in references [9,10], showing that the event sizes are broadly distributed according to a power law, which decays with an exponent roughly equal to 1.6 and spans various orders of magnitude. More recently, new acoustic emission experiments performed on more conventional metallic crystals such as Cd, Zn, or Cu under strain-controlled tensile tests show again the same phenomenology, scale free distributed plastic bursts or plastic avalanches with similar power law exponents [11]. The plastic flow of colloidal crystals at mesoscopic scales have also been analyzed by means of videomicroscopy [12]. A colloidal crystal made of charged polystyrene microspheres under stress induced by osmotic pressure gradients shows heterogeneous and intermittent dislocation behavior. The distribution of individual dislocation velocities appears to be quite broad as well as that of the global energy released through dislocation motion. The distribution of this last quantity appears to be well fitted by a power law with a similar exponent of 1.6. At microscopic scales, indentation experiments especially designed to perform compression tests on micron and submicron-sized single crystals of Ni exhibit large strain bursts and staircase strain-stress curves as well as highly fluctuating yield stress values as sample size is reduced [13,14]. The strain jumps in these strain-rate controlled experiments is again distributed according to a power law which decays with an exponent close to 1.6.

Despite some of the heterogeneous attributes concerning dislocation motion have been known for quite some time (for instance, their arrangement in intricate patterns inside the crystal, or the rough surface morphologies they give rise to through slip band formation), the most recent experimental findings emphasizing a certain degree of universality in the dislocation behavior have stimulated renewed interest in the subject. Universal behavior motivates and validates the formulation of simple models. These can help us unraveling the coarse-grained dynamics

of crystal plasticity, and the rich variety of physical phenomena emerging from the presence of topological defects in non-equilibrium conditions.

In this paper, we study several physical phenomena induced by the collective behavior of dislocations in simplified models of plastic deformation of crystals at mesoscopic scales. These models, that are mainly analyzed numerically, allow us to study the interplay between topological defects, geometry, and quenched disorder in the corresponding material. The paper is organized as follows. In Section 2 we first explore the collective dynamic behavior of a two-dimensional assembly of point-like edge dislocations with a discrete dislocation dynamics model. This mesoscopic approach has been widely used to study the mechanical behavior of conventional crystals such as metals and alloys, and will be very useful to investigate a dislocation mediated yielding transition in crystals undergoing plastic deformation. In particular, we will discuss the yielding transition between stationary and moving dislocation states, and the intermittent slow relaxations observed around this transition. Section 3 is devoted to the statistical analysis of the steady regime of plastic deformation achieved above the yielding threshold. We will show the occurrence of broadly distributed plastic avalanches in this simple model, avalanches that have also been measured in various experiments, in very recent numerical models in three dimensions [15] under various circumstances, as well as in the coarse grained model proposed in references [16,17] to study the dislocation yielding transition. In this section, we will comment their main characteristics and scaling behavior. We also study the temporal correlations of the strain-rate signal in the steady regime. These temporal correlations are quantified through the power-spectrum which scales as a power law of frequency. Its scaling properties are then justified in terms of the statistical properties concerning the size and duration of the plastic avalanches observed in this regime. The influence of the thresholding procedure used to identify avalanches is also discussed in this context. Finally, in Section 4 we draw the conclusions of our work.

2 Dislocation assemblies in two dimensions

A few years ago, we proposed a simple model to study the collective dynamics of a two-dimensional ensemble of point edge-like dislocations gliding along a unique gliding direction, i.e. a single slip system [9,18,19]. This model could represent, for instance, a cross section of a single slip crystal such as the ice single crystals referred above. The basic model incorporates the long range elastic interactions between dislocation pairs, with forces algebraically decaying as $1/r$ with distance r between dislocation pairs and changing sign according to the pair relative orientation, as well as dislocation pair annihilation and multiplication mechanisms (for details see Refs. [9,18,19]). Our main goal was to investigate the response of such a system under low stress driving conditions. For that purpose, we numerically solved the coupled equations of motion, assuming an overdamped dislocation dynamics and periodic

boundary conditions,

$$\frac{\chi_d^{-1} v_n}{b} = b_n \left(\sum_{m \neq n} \sigma^s(\mathbf{r}_{nm}) + \sigma \right), \quad (1)$$

where χ_d^{-1}/b is the effective friction per unit dislocation length and $\mathbf{r}_{nm} \equiv \mathbf{r}_n - \mathbf{r}_m$ the relative position vector of dislocations n and m . Indeed, an edge dislocation with Burgers vector $b\hat{x}$ located at the origin gives rise to a shear stress σ^s at a point $\mathbf{r} = (x, y)$ of the form

$$\sigma^s(\mathbf{r}) = Db \frac{x(x^2 - y^2)}{(x^2 + y^2)^2}, \quad (2)$$

where $D = \mu/2\pi(1 - \nu)$ is a coefficient involving the shear modulus μ and the Poisson ratio ν of the material.

These type of models, usually referred to as discrete dislocation dynamics models (DDD models) in the literature, are suitable to analyze the collective dislocation dynamics at mesoscopic lengthscales since they do not incorporate any of the microstructural changes undergoing in the crystal as dislocations move or pile against each other.

Starting from a random initial configuration of dislocations with Burgers vectors $\pm b\hat{x}$ pointing along the x axis, and after an initial period of free relaxation, dislocations glide and annihilate each other until they reach metastable configurations. At this point, the dislocation ensemble appears almost frozen. Most of the simulations were performed at *zero* temperature, although the influence of Gaussian thermal noise on the results was also explored. A constant stress σ was then applied to the relaxed dislocation configurations with the following results: a) If the stress value was well below a given threshold, we observed an initial time evolution of the average strain rate $\langle \dot{\gamma} \rangle$, followed by an exponentially fast relaxation towards zero strain rate. The strain rate is proportional to the density of mobile dislocations in each slip system and, for each numerical realization, we define it as

$$\dot{\gamma} = \sum_n b_n v_n, \quad (3)$$

where b_n and v_n are the Burgers vector and velocity of dislocation n along the glide direction x , respectively. This quantity is then averaged over many initial dislocation configurations. b) On the other hand, if the stress applied is above threshold the average strain rate reaches a stress-dependent plateau after a slow power-law relaxation, signaling a steady rate of plastic deformation. c) Close to the stress threshold the strain-rate decays as a power law with an exponent close to $2/3$ for all the time span [19,21]. In other words, plastic deformation in the model only occurs when the externally applied stress overcomes a threshold value σ_c , the yield stress of the material. Above this threshold, large-scale dislocation motion may take place and a steady regime of plastic deformation is established. Above σ_c the creep deformation curve could be well described by the general asymptotic behavior

$$\gamma(t) \sim \begin{cases} \beta t^{1/3} & \text{if } t < t_c \\ \dot{\gamma}_{st} t & \text{otherwise,} \end{cases} \quad (4)$$

where t_c is a characteristic crossover time whose value decreases with the external stress applied. The term $\beta t^{1/3}$ is known as Andrade creep, and the term $\dot{\gamma}_{st} t$ is referred to as linear creep regime. Both the coefficients β and $\dot{\gamma}_{st}$ depend on the external stress σ . The first term in equation (4) describes the linear but time dependent rheology of the dislocation assembly, β depends linearly on σ , and dominates at early times and for low applied stress values (see Fig. 1a). The last term describes a nonlinear steady flow, $\dot{\gamma}_{st}$ grows with the stress applied roughly like $\dot{\gamma}_{st} \sim \sigma^3$, and will be the main contribution at longer times and for higher stress values. In Figure 1 we summarize most of these findings. Here we have considered two system sizes of linear dimensions $L = 100b$ and $L = 300b$, containing 400 and 1500 initial dislocations, respectively. For both we obtain similar dynamic behavior around a threshold value $\sigma_c \sim 0.01$ (in the simulation units [20]) separating jammed and moving phases.

By analogy with the behavior of soft condensed matter systems, we could define a flow viscosity for the dislocation assembly in the moving phase as $\eta = \sigma/\dot{\gamma}$ resulting in a linear but time dependent viscosity $\eta(t) \sim t^{2/3}$ at short times, whereas at longer times it will crossover to a steady but nonlinear (shear thinning like) behavior $\eta_{st} \sim \dot{\gamma}_{st}^{-2/3}$. Both results appear to be coherent at least on dimensional grounds. Moreover, this result is compatible with the power law shear-thinning behavior $\eta \sim \dot{\gamma}^{-\alpha}$ with $\alpha = 0.5 - 1.0$ observed in many different complex fluids [22].

Similar results were obtained after considering various dislocation multiplication rates and thermal-like fluctuations. Dislocation multiplication favors the rearrangements of the system and induces a linear creep regime (flowing phase) at lower stress values, but it does not affect the initial power-law creep. The introduction of a finite effective temperature T has a similar effect [19].

Back in 1910 Andrade reported that the creep deformation of soft metals at constant temperature and stress grows in time according to a power law with exponent $1/3$ [23]. The same qualitative behavior has since been observed in many materials with rather different structures (including amorphous polymer melts or paper), leading to conclude that this should be a process determined by quite general principles. Nevertheless, this general behavior remains, as yet, unexplained. Most of the arguments used to explain Andrade's creep are based on thermally activated processes over time (or strain) dependent energy barriers. On the contrary, Andrade's creep has been observed to appear in the athermal version of this kind of simple model system, as well as in creep deformation experiments of paper, which suggest that the relaxation dynamics of residual stress in the vicinity of the yield threshold should be the relevant quantity to look at, the one responsible for such collective behavior.

The detailed analysis of the model data unveils the dislocation microscopic dynamics in the Andrade and the stationary regimes: Most dislocations are arranged into metastable structures so that the stress field generated in the material is screened out on large length-scales.

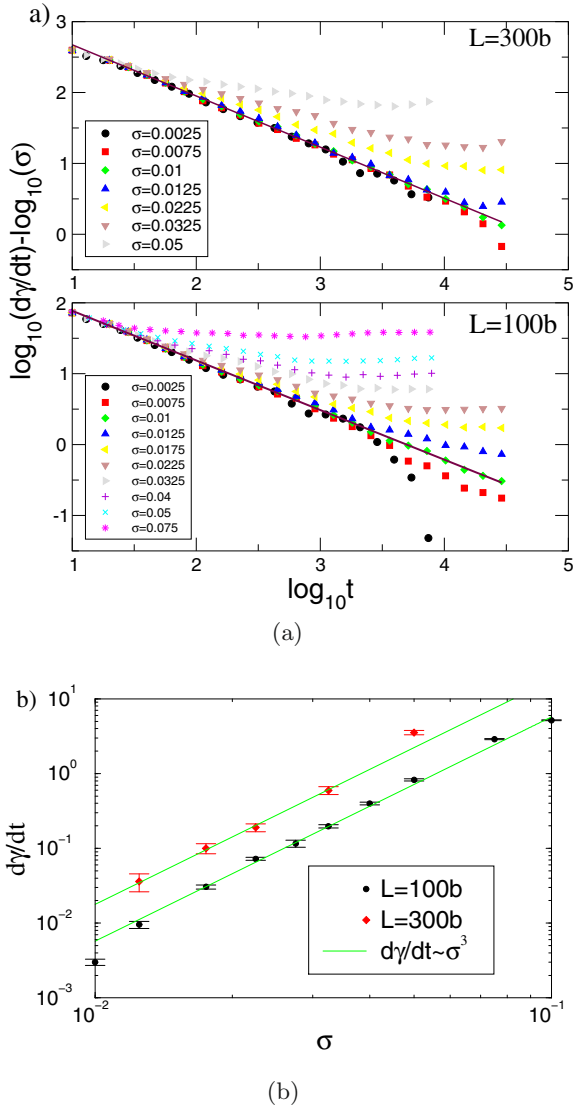


Fig. 1. a) Time evolution of the average strain rate after the application of external stress σ to relaxed dislocation configurations without creating new dislocation pairs. The applied stress ranges between $\sigma = 0.0025 - 0.1$ in the simulation units [20]. The solid line represents the best linear fit of the $\sigma = 0.01$ strain-rate curve for two system sizes of linear dimensions $L = 100b$ and $L = 300b$. b) Strain rate versus stress relation in the steady state. The solid lines represent a cubic law. The average strain-rate depends on the initial dislocation densities which change with L .

These structures consist of small-angle dislocation boundaries separating slightly misoriented crystalline blocks or far more complex dislocation arrangements. If the applied stress is below the yield threshold, dislocations are unable to explore the space of configurations looking for more favorable arrangements and they are, most of the time, trapped in metastable configurations, which induce a jamming of the system. In Figure 2a, we show a snapshot of the dislocations and the shear stress distribution within the jammed phase. The stress applied is 0.005 in the simulation units [20], that is below the yield threshold for

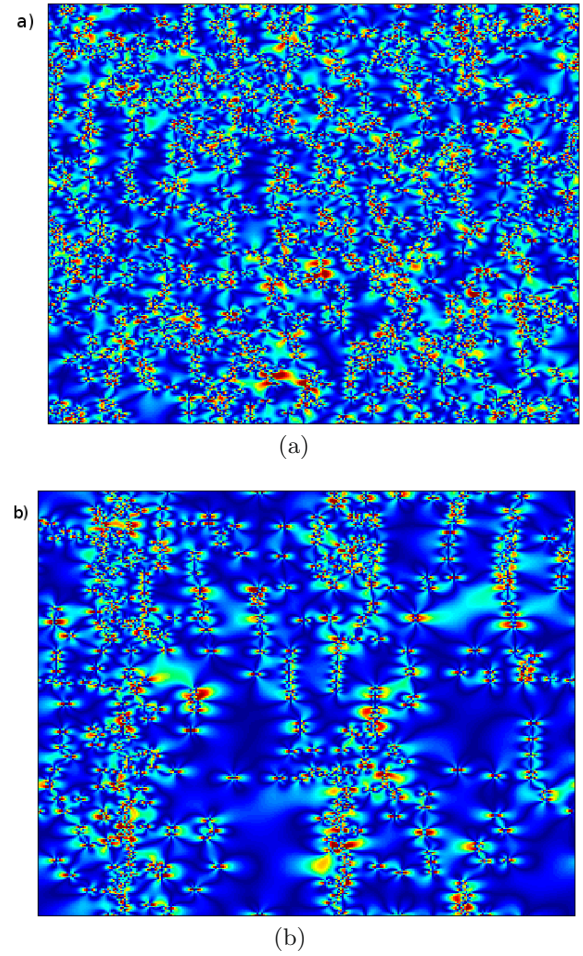


Fig. 2. Snapshots representing the dislocation configurations and the residual shear stress in a jammed phase with $\sigma = 0.005$ (top) and in the moving phase for $\sigma = 0.07$ (bottom) [20]. The system size considered here is $L = 300b$. Internal stress levels are represented with different colors from dark blue (lowest stress) to dark red (highest stress).

$L = 300b$. Internal stress levels are represented with different colors from dark blue (lowest stress values) to dark red (highest stress values). Around the yield threshold, a small fraction of dislocations may, however, attain a higher mobility and provoke several intermittent rearrangements of the whole system in the course of time. The shear stresses generated by these unsettled dislocations conserve the initial long-range character and force the system to continue evolving in time, in a cooperative manner, to try to screen them out (or minimize the internal energy) by exploring further more favorable arrangements. Figure 2b shows one example of a moving configuration for $\sigma = 0.07$, including the corresponding shear stress distribution.

Furthermore, in Figure 3, we also show the mean kinetic energy $N\langle v^2 \rangle = \sum_i v_i^2$ of all the dislocations present in a square cell of size $L = 100b$ as a function of time for a single run of the numerical simulations (initially, $N = 121$ dislocations). Each run would represent the creep behavior of a small piece (a few nanometers big) of a macroscopic system, and starts from different initial dislocation

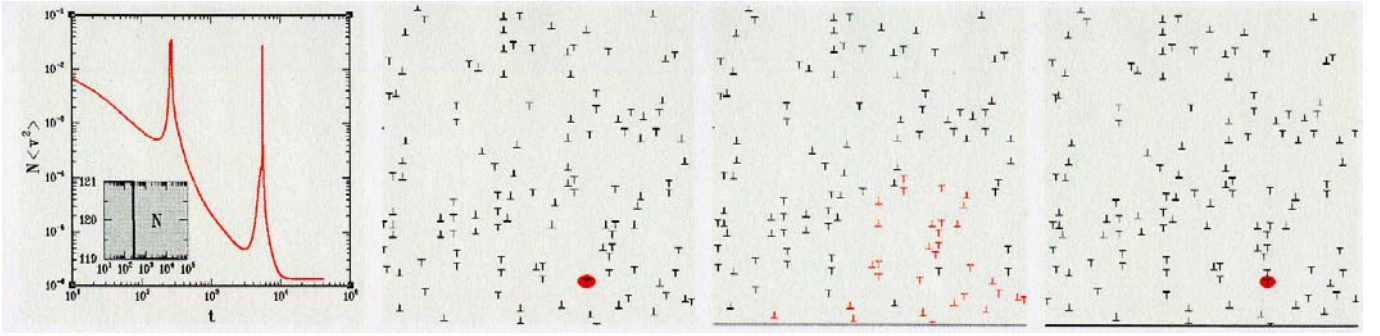


Fig. 3. Time evolution of the mean kinetic energy in a single simulation run without creation of new dislocations (left). Here the applied stress is $\sigma = 0.0125$ and the system size $L = 100b$ [20]. Three snapshots illustrating the arrangement of dislocations before the second spike (left), at the second peak maximum (center), and after the peak (right). The dislocation marked with a red circle in the first and last snapshots has finally become part of a dislocation wall after a collective dislocation rearrangement (red dislocations within the central snapshot).

configuration obtained after letting the system relax in the absence of external load during a given time interval. The external shear stress applied in this case is $\sigma = 0.0125$, that is, in the vicinity of the critical threshold around $\sigma_c \sim 0.01$ for the system sizes considered $L = 100b$ and $L = 300b$. We can clearly appreciate the presence of intermittent bursts after which $\langle v^2 \rangle$ slowly decreases in time. The first burst is clearly triggered by the annihilation of a dislocation pair, as can be corroborated in the inset of the figure showing the evolution of the number of dislocations in the run. The second burst is, on the other hand, triggered by the collective dislocation rearrangement illustrated with three snapshots recorded before (left), at the peak maximum (center), and after (right) the rearrangement has taken place. Black dislocations have a velocity below the external stress induced velocity, which in the simulation units is equal to $\sigma = 0.0125$. Red dislocations (second snapshot) are moving with a higher velocity. After the second velocity burst, one dislocation, marked in red in both the initial and final snapshots, that initially was separated from a dislocation wall has finally become part of the wall. A collective rearrangement (highlighted by red color dislocations within the central snapshot) has made that possible. Similar bursts, but either positive or negative, can also be observed in the corresponding strain-rate curves $d\gamma/dt$. Andrade’s power law creep appears as a result of the averaging process over many of these runs, mimicking the behavior of a much bigger system.

3 Stress-strain curves and plastic avalanches in the steady state

In the flowing state, but close to the yielding transition the dynamics of the dislocation assembly can be characterized by a combination of incoherent small-scale motions and collective avalanches. Dislocation avalanches have been identified in several experiments at various size scales and for different deformation protocols (creep,

load-controlled or strain-controlled tests) [8–14]. Similarly, plastic avalanches have been revealed in numerical simulations in two [9,16–18] and, more recently, in three dimensions [15]. All these simulations try to incorporate the most essential features characterizing dislocation interactions and motion. After thresholding the strain-rate signal to eliminate incoherent small-scale motions (or numerical noise) and to identify dislocation avalanches, the size distribution of the resulting plastic bursts have demonstrated to show a very robust scaling behavior with size s as $s^{-\tau_s}$ with an exponent τ_s close to 1.6, in close agreement with most of the experimental results. The spatiotemporal characterization of this steady state proceeds by showing that they are indeed separate avalanches, and concentrates on the most pertinent signatures of the steady state.

3.1 Scaling of the power spectrum of yielding

Here we compute the power spectrum (PS) of the global dislocation velocity $V(t) = \sum_i |v_i|$. This is an intermittent signal consisting of plastic avalanches on top of a background due to incoherent dislocation motion. An example of such a time series is shown in Figure 4. Our recent results [24] indicate that in addition to the power law distribution characterizing the avalanches (which are identified after thresholding the signal $V(t)$ with some threshold value V_{th}), the high frequency part of such a PS can also be described by a power law, $P(f) \sim 1/f^\alpha$, with a non-trivial exponent α . For $0 < \alpha < 2$, this is usually referred to as $1/f$ noise. Furthermore, one can understand the origin of the exponent α , as it can be related to the exponents describing the avalanches [24]. This appears to be a generic property of “critical” avalanching systems, examples ranging from models of Barkhausen noise [25] to self-organized criticality [26] to fluctuations in fluid invasion into disordered media [27].

The scaling relation connecting the scaling of the PS to that of the avalanches is obtained by assuming that the avalanches have an average *shape* described by a function

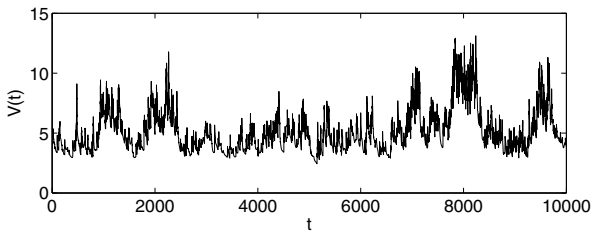


Fig. 4. An example of a time series $V(t) = \sum_i |v_i|$, displaying intermittent bursts or avalanches of dislocation activity.

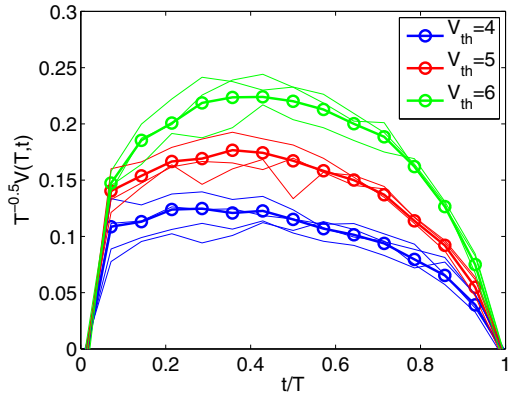


Fig. 5. A scaling plot displaying the average avalanche shape for various threshold values V_{th} for $\sigma = 0.03$ and $L = 300b$. The thick solid lines with circular symbols correspond to an average over the order of 10^3 avalanches, which have been scaled according to equation (5) before averaging. The thin solid lines correspond to avalanches of different limited duration ranges. Notice the asymmetry in the avalanche shapes.

$f_{shape}(x)$, such that the averaged avalanche shapes $V(T, t)$ of avalanches of different durations T can be collapsed onto a single curve by using the ansatz

$$V(T, t) = T^{\gamma_{st}-1} f_{shape}(t/T), \quad (5)$$

where γ_{st} is the exponent relating average avalanche size $\langle s(T) \rangle = \langle \int_0^T [V(t) - V_{th}] dt \rangle$ and duration T through $\langle s(T) \rangle \sim T^{\gamma_{st}}$. By averaging the energy spectrum of avalanches of size s over the avalanche size probability distribution $D_s(s) \sim s^{-\tau_s}$ (see Ref. [24]), one finds that for $\tau_s < 2$, the PS scales as

$$P(f) \sim f^{-\gamma_{st}}, \quad (6)$$

i.e. $\alpha = \gamma_{st}$. This relation has been verified numerically, resulting in $\alpha = \gamma_{st} \approx 1.5$ for the model at hand, see Figure 6. The observed scaling seems to be largely independent of the value of the external stress, as well as many other details of the model, such as the precise mechanism to create new dislocation pairs. Similar results can be recovered even in the case with no dislocation multiplication, where avalanches are due to different threshold mechanisms such as depinning of dislocation dipoles.

Notice that the above scaling relation assumes that correlations between different avalanches are negligible, such that the $1/f^\alpha$ decay of the PS reflects correlations

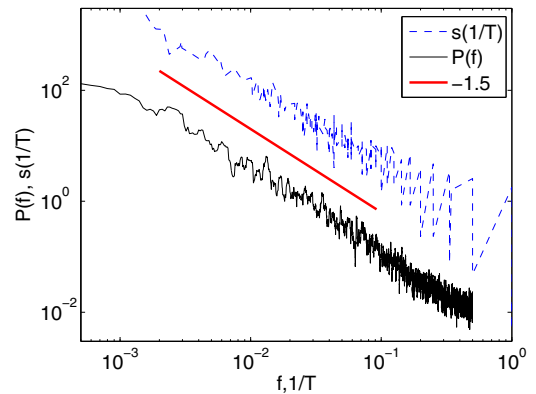


Fig. 6. Scaling of the power spectrum of $V(t)$ and the average avalanche sizes for $\sigma = 0.03$ and $L = 300b$. The thick solid line corresponds to $\alpha = \gamma_{st} = 1.5$.

within individual avalanches only. In experiments, however, dislocation avalanches have been found to exhibit a tendency to cluster in time ([28] as well as the next subsection on waiting time distributions). This could modify the low-frequency part of the PS (indeed we do not observe an abrupt crossover to white noise behavior for low frequencies), but the high frequency part (i.e. frequencies higher than the one corresponding to the inverse duration of the longest avalanche) should still be dominated by correlations within individual avalanches and thus follow the scaling of equation (6).

Another important condition for equation (6) is the existence of a “universal” avalanche shape, equation (5). For the present case in which we are considering a simplified model of a single crystal, this seems to be true for large enough avalanches. For polycrystals, however, this is not necessarily the case: Large avalanches tend to interact with the grain boundaries, leading most likely to an s -dependent $f_{shape}(x)$ [10]. Interestingly, the average avalanche shape observed in the present case appears to be asymmetric in time, see Figure 5. This is in line with results from acoustic emission experiments [29]. In Barkhausen noise, an explanation for the pulse shape asymmetry involves a negative mass term in the dynamical equation for the avalanche activity [30]. The applicability of such a coarse-grained description is not clear for dislocation avalanches, but the idea needs to be investigated in the future.

Similar scaling for the power spectra have been observed also in other systems in which dislocation or grain boundary motion takes place, for instance, in the vortex lattice of a type II superconductor in the mixed phase. There the nucleation and motion of topological defects in the vortex crystal gives rise to similar scaling properties of the resistance noise power spectra [31,32].

3.2 Coherent and incoherent dynamics

Next we illustrate the intermittent character of the flowing state by considering how to separate the “true avalanches” from the rest in $V(t)$. First, as for the $1/f$ -spectrum, let us

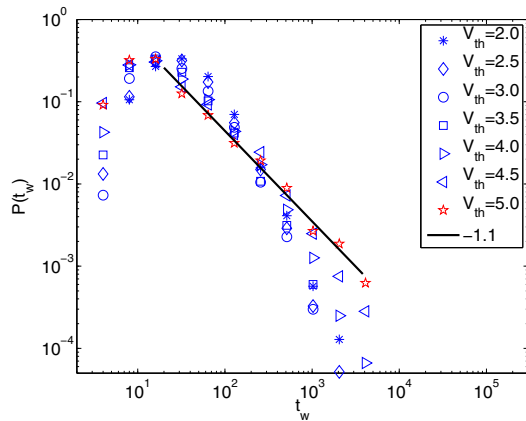


Fig. 7. The distribution of waiting times, defined here as the time intervals between two consecutive avalanche triggerings, for various V_{th} -values, with $L = 200b$ and $\sigma = 0.03$. In order to eliminate the effect of noise, only avalanches of size $s > 5$ are considered. The solid line corresponds to a power law with an exponent -1.1 .

look at the result of splitting the signal into avalanches by thresholding by V_{th} . This will create a sequence of waiting times t_w , defined as the time interval between two consecutive avalanche triggerings (the instant when $V(t)$ crosses V_{th} from below).

The distributions of such quantities can be used to quantify the correlations between subsequent avalanches, and have in general been considered as signatures of correlations in driven, out-of-equilibrium systems [33]. Here, the triggering of an avalanche from a quiescent state starts from the low-level incoherent state of activity. If the triggerings of different avalanches are not correlated, the process is expected to be related to a Poisson process, corresponding to an exponential distribution of waiting times. Thus, deviations from the exponential law are a sign of correlation between different avalanches.

Figure 7 shows the waiting time distributions for a system in the moving steady state, with $L = 200b$ and $\sigma = 0.03$. Other external stress values yield similar results close but above σ_c . The distribution clearly evolves with the threshold applied so that as the threshold V_{th} is increased, two waiting times are joined, as well as the duration of any event in between. For sufficiently high threshold values V_{th} , the distributions $P(t_w)$ follow a power law, $P(t_w) \sim t_w^{\tau_w}$. The exponent τ_w is observed to be close to -1 . The power law waiting time distribution is in qualitative agreement with experimental evidence of avalanche correlations [28].

The presence of inter-avalanche correlations can also be detected by computing the correlation integral of avalanche starting times (Fig. 8). Here, we can see the effect of V_{th} in that a high value will break into sub-avalanches larger ones, thus creating clusters of highly correlated avalanches and a small correlation dimension (slope of the integral). For low thresholds, the correlation dimension is observed to be only slightly below unity (about 0.9), but upon increasing V_{th} , significant clustering of avalanche starting times is observed.

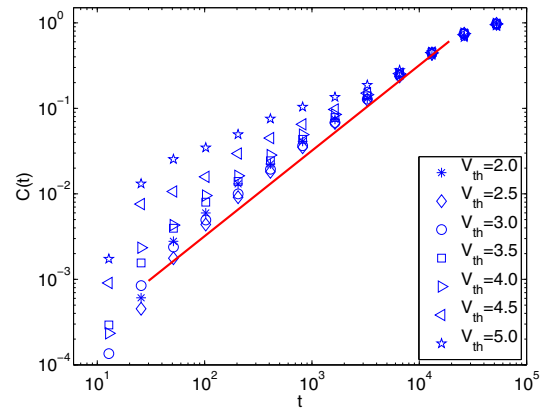


Fig. 8. Correlation integral of avalanche starting times for various V_{th} -values.

4 Conclusions

Here we have reviewed the physics of dislocation dynamics close to the yielding transition. The change from a frozen, “jammed” state to a moving one appears to be a second-order phase transition, and it results in these systems from a combination of long-range anisotropic interactions and topological constraints.

The physics of the jamming transition must thus be linked to the formation of dislocation structures and it remains an open question what message this tells about the universality or possible universality classes - what the dependence of the critical properties would be on the details of the model at hand. It is worth pointing out the similarities and differences with another class of absorbing state phase transitions: pinning and depinning. The models we have considered here do not include any external (quenched) randomness, that would couple to coarse-grained elastic degrees of freedom and the externally applied stress. The coarse-grained description of the dislocation systems here might be conjectured to have a *self-organized* spatially varying, random force field coming from the fluctuating effect of dislocation structures [16,17]. It would thus seem to be an interesting issue to study the formation of dislocation structures close to the yielding/jamming transition.

Another crucial feature of the physics here is that we are usually considering the dynamics in the absence of thermal noise. It is an interesting question as to what this tells then us about the general physics of creep deformation, in particular the fact that the models reproduce “primary creep” or an Andrade law. Clearly here this does not result from any thermally activated dynamics of dislocations or deformation. The fact that the dislocation assemblies close to the yielding transition exhibit strong history dependence brings forth further interesting analogies with the time-dependent mechanics of materials. Figures 9 show two examples of the effect produced by two different load histories on the deformation dynamics. The dislocation assemblies are submitted to several loading/unloading cycles of creep deformation with constant stress. The system is unloaded during the same period

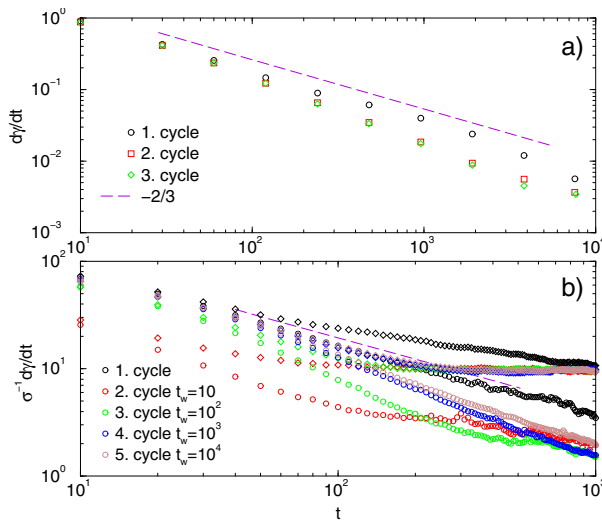


Fig. 9. Time evolution of the average strain rate for fatigue-like creep tests, i.e. loading/unloading cycles with constant stress σ . a) $\sigma = 0.01$. Unloading cycles of equal duration $t_w = 5 \times 10^3$. b) Unloading cycles of different durations $t_w = 10, 10^2, 10^3, 10^4$. Two different external stress values are considered: $\sigma = 0.01$ (circles) and $\sigma = 0.04$ (diamonds).

($t_w = 5 \times 10^3$ time units) in Figure 9a, or during different waiting times ($t_w = 10, 10^2, 10^3, 10^4$ time units) in Figure 9b. The primary regime of slow relaxation as well as the crossover time to the steady regime are clearly influenced by the deformation history. The relaxation of internal stress over the time intervals with no load (aging periods) results in a non trivial response of the system which has to be further explored [34]. Nevertheless, these suffice to demonstrate that these models, hence maybe many real crystalline materials, also exhibit waiting-time dependent response.

In summary, the materials science-inspired particle models of dislocation assemblies present novel problems for statistical physics, and offer interesting analogies with the physics of jamming transitions in granular media. They also highlight the benefits of trying to understand the hitherto often neglected intermittent character of deformation in materials science, in particular the crackling noise that ensues therein.

We would like to thank S. Zapperi, P. Moretti, M. Zaiser, J. Weiss, and A. Vespignani for their collaboration and valuable discussions on the general subject over the last years. MCM acknowledges financial support from the Spanish Ministerio de Educación y Ciencia (FIS2004-05923-CO2-02), and from the Generalitat de Catalunya (Distinció). MCM is also very grateful to the Helsinki University of Technology for providing additional support during the summer visit to the Laboratory of Physics where most of this writing was carried out. LL wishes to thank MCM and Universitat de Barcelona for hospitality. LL and MJA would like to acknowledge the support of the Center of Excellence -program of the Academy of Finland and the European Commissions NEST Pathfinder programme TRIGS under contract NEST-2005-PATH-COM-043386.

References

1. *Jamming and Rheology*, edited by A.J. Liu, S.R. Nagel, (Taylor and Francis, London, 2001)
2. C.S. O'Hern, S.A. Langer, A.J. Liu, S.R. Nagel, *Phys. Rev. Lett.* **88**, 75507 (2002)
3. C.S. O'Hern, L.E. Silbert, A.J. Liu, S.R. Nagel, *Phys. Rev. E.* **68**, 011306 (2003)
4. *Jamming, Yielding and Irreversible Deformation in Condensed Matter*, Lect. Notes Phys. **688**, edited by M.C. Miguel, J.M. Rubí (Springer, Berlin Heidelberg, 2006)
5. J. Lauridsen, M. Twardos, M. Dennin, *Phys. Rev. Lett.* **89**, 098303 (2002)
6. O. Dauchot, G. Marty, G. Biroli, *Phys. Rev. Lett.* **95**, 265701 (2005)
7. A.S. Keys, A.R. Abate, S.C. Glotzer, D.J. Durian, *Nature Phys.* **3**, 260 (2007)
8. J. Weiss, J.R. Grasso, *J. Phys. Chem. B* **101**, 6113 (1997)
9. M.-C. Miguel, A. Vespignani, S. Zapperi, J. Weiss, J.R. Grasso, *Nature* **410**, 667 (2001)
10. T. Richeton, J. Weiss, F. Louchet, *Nature Materials* **4**, 465 (2005)
11. T. Richeton, P. Dobron, F. Chmelik, J. Weiss, F. Louchet, *Mater. Sci. Eng. A* **424**, 190 (2006)
12. A. Pertsinidis, X.S. Ling, *New J. Phys.* **7**, 33 (2005)
13. M.D. Uchic, D.M. Dimiduk, J.N. Florando, W.D. Nix, *Science* **305**, 986 (2004)
14. D.M. Dimiduk, C. Woodward, R. LeSar, M.D. Uchic, *Science* **312**, 1188 (2006)
15. F.F. Csikor, C. Motz, D. Weygand, M. Zaiser, S. Zapperi, *Science* **318**, 251 (2007)
16. M. Zaiser, P. Moretti, *J. Stat. Mech.: Theory Exp.*, P08004 (2005)
17. M. Zaiser, *Adv. Phys.* **55**, 185 (2006)
18. M.C. Miguel, A. Vespignani, S. Zapperi, J. Weiss, J.R. Grasso, *Mater. Sci. Eng. A* **309-310**, 324 (2001)
19. M.C. Miguel, A. Vespignani, M. Zaiser, S. Zapperi, *Phys. Rev. Lett.* **89**, 165501 (2002)
20. Lengths are measured in units of the annihilation distance y_a , time in units of $t_0 = y_a^2/(\chi_d D b^3)$, and stress in units of $\sigma_0 = D b/y_a$
21. M.C. Miguel, P. Moretti, M. Zaiser, S. Zapperi, *Mater. Sci. Eng. A* **400-401**, 191 (2005)
22. R.G. Larson, *The Structure and Rheology of Complex Fluids* (Oxford University Press, New York, 1999)
23. E.N. da C. Andrade, *Proc. R. Soc. London A* **84**, 1 (1910)
24. L. Laurson, M.J. Alava, *Phys. Rev. E* **74**, 066106 (2006)
25. M.C. Kuntz, J.P. Sethna, *Phys. Rev. B* **62**, 11699 (2000)
26. L. Laurson, M.J. Alava, S. Zapperi, *J. Stat. Mech.* L11001 (2005)
27. M. Rost, L. Laurson, M. Dubé, M. Alava, *Phys. Rev. Lett.* **98**, 054502 (2007)
28. J. Weiss, M.C. Miguel, *Mat. Sci. Eng. A* **387-389**, 292 (2004); **309-310**, 360 (2001)
29. T. Richeton, J. Weiss, F. Louchet, *Acta Mater.* **53**, 4463 (2005)
30. S. Zapperi, C. Castellano, F. Colaioni, G. Durin, *Nature Physics* **1**, 46 (2005)
31. G. Jung, private communication and contribution in Ref. [4]
32. M.C. Miguel, S. Zapperi, *Nature Materials* **2**, 477 (2003)
33. M. Paczuski, S. Boettcher, M. Baiesi, *Phys. Rev. Lett.* **95**, 181102 (2005)
34. B. Bakó, I. Groma, G. Györgyi, G. T. Zimányi, *Phys. Rev. Lett.* **98**, 075701 (2007)